CRYSTAL GROWTH & DESIGN

Article

pubs.acs.org/crystal

Screw Dislocation-Driven Growth of the Layered Spiral-type SnSe Nanoplates

Jinyang Liu,*[,†,‡,§] Qingqing Huang,[†] Yongqiang Qian,[†] Zhigao Huang,[†,‡,§] Fachun Lai,[†,‡,§] Limei Lin,[†,‡,§] Mingzhu Guo,[†] Weifeng Zheng,[†] and Yan Qu[†]

[†]College of Physics and Energy, Fujian Normal University, Fuzhou 350117, P. R. China

[‡]Fujian Provincial Key Laboratory of Quantum Manipulation and New Energy Materials, Fuzhou 350117, P. R. China

[§]Fujian Provincial Collaborative Innovation Center for Optoelectronic Semiconductors and Efficient Devices, Xiamen 361005, P. R. China

ABSTRACT: A high degree of control over thickness, size, structure, and symmetry of two-dimensional layered materials is essential to tune their chemical and physical properties for applications. Here, we report screw dislocation-driven growth of layered spiral-type SnSe nanoplates with atomically thin helical periodicity for the first time. The spirals are composed of a few connected SnSe layers with decreasing areas; each basal plane has a rectangular shape and spirals up layer by layer to the summit center. The unique structure and growth mode were further confirmed to include herringbone contours, spiral arms, and hollow cores. In addition, the growth mode can be tuned from screw dislocation-driven growth to layer-by-layer growth by manipulating the precursor concentration. The results shown here may provide valuable guidance for the design and growth of unique nanostructures in SnSe or even other two-dimensional layered materials and promote their applications.

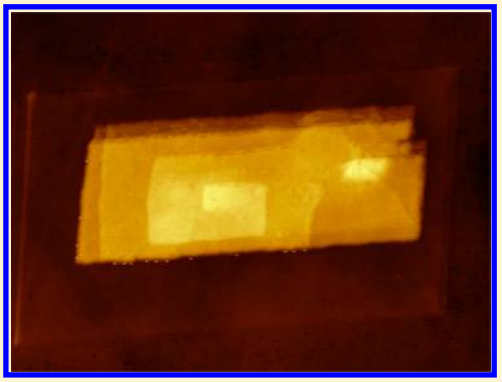

1. INTRODUCTION

Atomically thin two-dimensional (2D) layered materials, including graphene, boron nitride (BN), and transition metal dichalcogenides (TMDs), exhibiting novel phenomena distinguished from their bulk counterparts hold great promise for novel electronic and optoelectronic applications.[1,2] Controlled growth of such 2D materials with different thickness, size, structure, symmetry and composition are extremely challenging but highly desirable in scientific research. Among various 2D layered materials, atomically thin IV−VI binary semiconductors, such as SnS, SnSe, GeS, and GeSe, demonstrating unique electronic structures and physical properties have become a hot spot of recent research.[3−5] In particular, as an important p-type semiconductor, SnSe has attracted intense attention in solar cells, photodetectors, and near-infrared optoelectronic devices due to its narrow band gap (~0.90 eV indirect and ~1.30 eV direct), earth-abundance, low toxicity, and chemical stability.[6−8] To date, various shapes of SnSe nanostructures have been synthesized, including SnSe nanowires,[9] SnSe nanosheets,[10] SnSe nanoflowers,[11] and so on. However, some unique structures, including atomically thin spiral-type SnSe layered nanostructures, are rarely studied.

Screw dislocation-driven (SDD) growth was predicted by classical crystal-growth theory, which is distinguished from the other two basic growth modes, namely, layer-by-layer (LBL) growth and dendritic growth, in terms of the supersaturation conditions.[12] In high supersaturation, the LBL and dendritic growth modes are activated. In contrast, at very low supersaturation, only SDD growth is permitted, and the products may contain novel properties due to their anisotropic growth, which has gained a lot of attention recently.[12,13] As a matter of fact, one-dimensional (1D) nanowires (NWs)[14−17] and nanotubes (NTs),[18−20] and even three-dimensional (3D) nanotrees,[21−23] were systematically investigated upon being driven by the SDD growth mechanism. However, 2D nanomaterials such as nanoplates and nanosheets, grown by the SDD mechanism are rarely reported and only come to pass in a few cases, including hydroxy sulfate and Au nanoplates.[24] Thereafter, it is natural to extend the SDD growth mechanism to the 2D layered materials, which are in an entirely different category and have attracted increasing attention. In fact, the spiral-type MoS_2, WSe_2, and SnS_2 grown via chemical vapor deposition[25−27] and Bi_2Se_3 nanoplates[28] via nonaqueous solution synthesis have been realized. However, all of these belong to the hexagonal crystal system;[24−26,28,29] SDD growth rarely extends to other crystal structures, such as in the orthorhombic crystal system.

In this report, we demonstrated SDD growth of the layered spiral-type SnSe nanoplates with atomically thin helical periodicity. The spirals are composed of a few connected SnSe layers with decreasing areas; each basal plane has a rectangular shape and spirals up layer by layer to the summit

Received: December 2, 2015
Revised: March 5, 2016

DOI: 10.1021/acs.cgd.5b01708
Cryst. Growth Des. XXXX, XXX, XXX−XXX

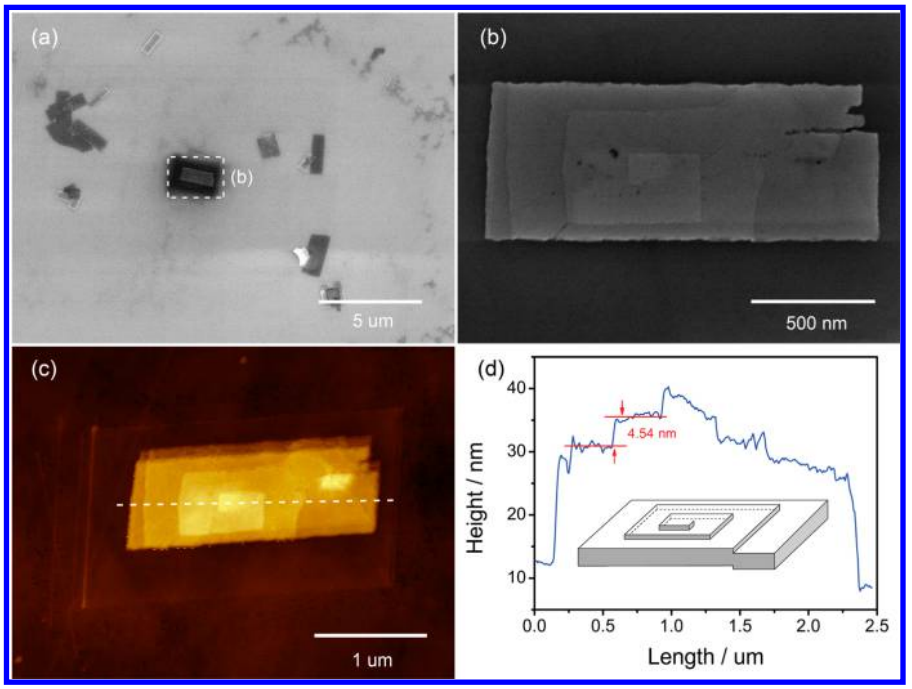

Figure 1. (a) Low-magnification SEM image of SnSe nanoplates obtained from a standard synthetic procedure. (b) High-magnification SEM image of a representative layered spiral-type SnSe nanoplate shown in (a) with a dashed square. (c) AFM amplitude image of the nanoplate. (d) AFM height profile of the nanoplate along the dashed white line in (c). The inset is a schematic representation of the incorporation of screw dislocation into the layered structure of SnSe.

center. The unique structure and growth mode of the layered spiral-type SnSe nanoplates were characterized by SEM, AFM, TEM, and EDS, which further confirmed that herringbone contours, spiral arms, and hollow cores also exist. In addition, we further tuned the SDD growth mode to the layer-by-layer growth mode by manipulating the precursor concentration to prove the classical crystal growth theory. The results shown here may provide valuable instructions for designing and growing spiral-type atomically thin IV−VI binary semiconductors, which could even extend to other 2D layered materials.

2. EXPERIMENTAL SECTION

Chemicals. All chemical materials were of analytical grade and used as received without further purification. Tin(II) chloride dihydrate ($SnCl_2{\cdot}2H_2O$, ≥98%), polyvinylpyrrolidone (PVP, 99.0%), and benzyl alcohol (≥98%) were purchased from Tianjing Fuchen Chemical Reagents Factory. Selenium dioxide (SeO_2, 99.9%) was obtained from Chengdu Ai Keda Chemical Technology Co., Ltd. Some common organic solvents (ethanol and others) were of analytical grade and obtained from Sinopharm Chemical Reagent Co., Ltd.

Synthesis of the Layered Spiral-type SnSe Nanoplates. In a typical synthesis of the layered spiral-type SnSe nanoplates, $SnCl_2{\cdot}2H_2O$ (0.8 mmol/L), SeO_2 (0.8 mmol/L), and poly(vinylpyrrolidone) (PVP, 0.32 g/mL) were added to benzyl alcohol (20 mL) at room temperature. Then, the mixed solution was transferred into a three-neck round-bottom flask, sealed, and then degassed with pure N_2 (99.99%) under magnetic stirring. Then, the mixture was heated to 200 °C and allowed to age for another 12 h at this temperature in a N_2 atmosphere. Finally, the solution was cooled to room temperature naturally, and the product was obtained by centrifugation at 10000 rpm for 10 min. The products were additionally purified at least twice by resuspending them in absolute alcohol. The products could then be well-resuspended in ethanol for further characterization.

Characterization. Raman spectroscopy was recorded at room temperature using HORIBA Jobin Yvon Evolution with laser excitation at 532 nm with power less than 5 mW. The UV−vis−NIR was characterized by a Perkin Elmer Lambda 950 spectrophotometer. Scanning electron microscopy (SEM) was characterized by a Hitachi SU-8010 microscope. Atomic force microscopy (AFM) was characterized by an Agilent 5500 microscope. Powder X-ray diffraction (XRD) patterns were characterized by PANalytical X'Pert ProMPD (Cu Kα, λ = 0.15418 nm). Transmission electron microscopy (TEM) with selected area electron diffraction (SAED) was characterized by JEOL JEM-2010 transmission electron microscope. Element analysis was recorded by energy-dispersive X-ray spectroscopy (EDX, AMETEK) attached to the transmission electron microscope.

3. RESULTS AND DISCUSSION

The as-synthesized nanocrystals were first characterized by SEM, and the typical results are shown in Figure 1 (a, b). The majority of products were rectanglar and platelike with a typical lateral size of 1−2 um. Through detailed examination of the samples, it can be found that they all contained helical fringes on the surfaces. Figure 1 (b) shows the high-magnification SEM image of a representative individual nanoplate masked with a white box in Figure 1 (a); it can been seen that the nanoplate contains a single helical pattern and a helical core located at the center. Overall, they look like pyramids; each basal plane has a rectangular shape and gradually shrinks to the center summit layer by layer when spiraling up. Thus, the as-synthesized SnSe nanocrystals are called layered spiral-type SnSe nanoplates for simplicity. The layered spiral-type SnSe nanoplates are the first spiral-type 2D layered material discovered other than the hexagonal crystal system[24−26,28,29] reported previously, and it may provide useful instruction for the generation of other crystal systems.

For the detailed structures to be explored further, the layered spiral-type SnSe nanoplates shown in Figure 1 (b) were carefully investigated by atomic force microscopy (AFM), and the corresponding results are shown in Figure 1 (c). AFM characterization shows that the layered spiral-type SnSe

DOI: 10.1021/acs.cgd.5b01708
Cryst. Growth Des. XXXX, XXX, XXX−XXX

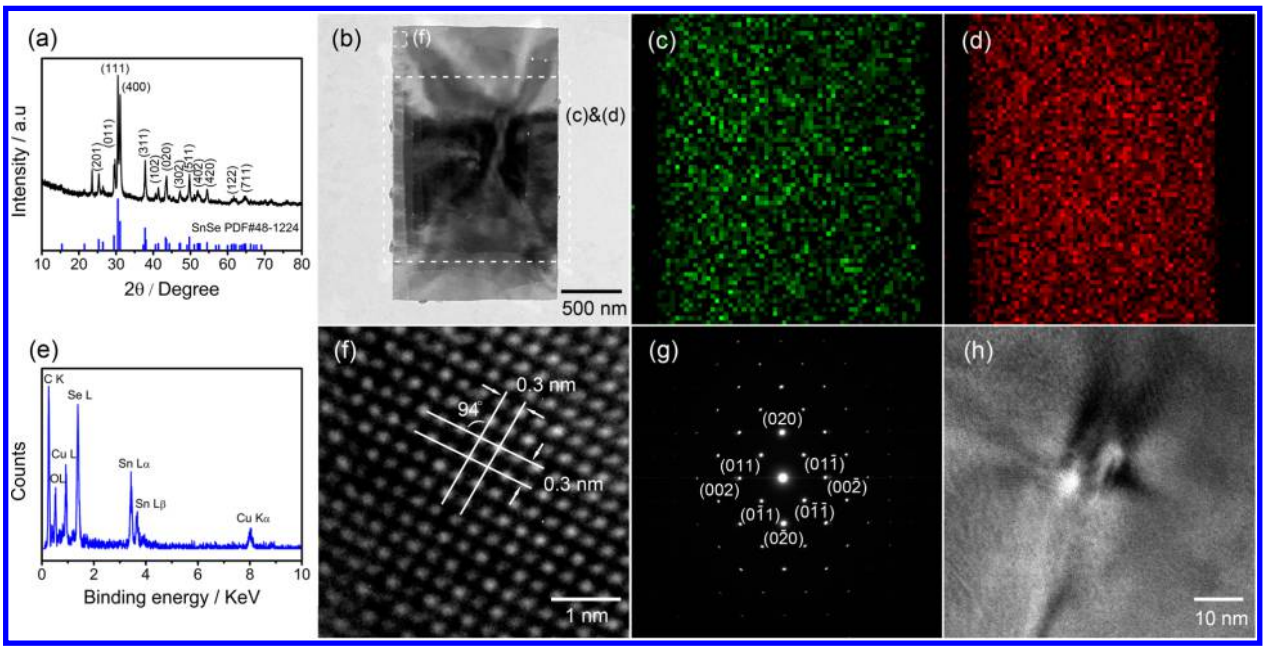

Figure 2. (a) Powder XRD pattern of the layered spiral-type SnSe nanoplates. (b) Low-magnification TEM image of the representative layered spiral-type SnSe nanoplates. (c, d) Sn and Se elemental maps of the corresponding SnSe nanoplates, respectively, shown in the rectange in (b). (d) EDX spectrum of the layered spiral-type SnSe nanoplates. (f) High-magnification TEM image of the representative layered spiral-type SnSe nanoplates of the rectange in (b). (g) SAED pattern of the layered spiral-type SnSe nanoplates. (h) Magnified TEM image of the center region of the nanoplate of (b).

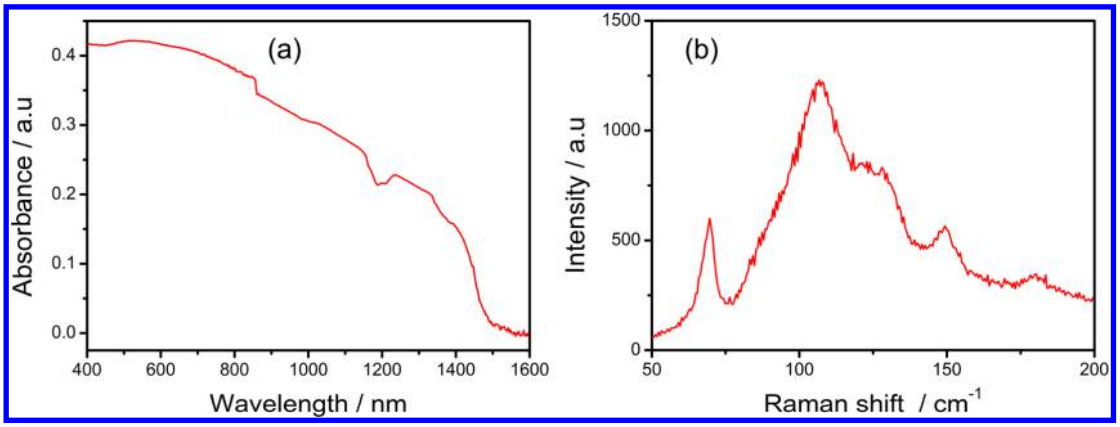

Figure 3. (a) Typical absorption spectrum of the layered spiral-type SnSe nanoplates dispersed in ethanol. (b) Raman spectrum of the layered spiral-type SnSe nanoplates.

nanoplates look like pyramids with a thickness of approximately 35 nm, and each basal plane has a rectangular shape. In addition, the spiral arms are clearly observed and spiral up layer by layer to the center summit; consequently, helical fringes are exhibited distinctly. Furthermore, the height of the step is approximately 4.5 nm as indicated from the cross-section height profiles shown in Figure 1 (d). It can been concluded that the thin flakes are approximately 4 layers due to the thickness of the monolayer SnSe being approximately 1 nm.[11] For the screw dislocations to be described more clearly, a schematic model was drawn as shown as an inset to Figure 1 (d). As is known, SnSe has an orthorhombic crystal structure in space group *Pnma* (62), which can be regarded as a severely distorted NaCl structure with atoms arranged in two adjacent double layers of tin and selenium, forming a planar bilayer (BL) structure and held together by weak van der Waals interactions.[7,10] The incorporation of screw dislocation into orthorhombic SnSe can presumably transform the layered structure into a continuous spiral belt and thus create a drastically different type of platelike SnSe material. Therefore, the layered spiral-type SnSe nanoplates, as a new type of atomically thin two-dimensional (2D) layered material, may have great promise in applications for novel electronics and optoelectronics.

The powder X-ray diffraction (XRD) pattern is performed to elucidate the phase structure of the layered spiral-type SnSe nanoplates. As shown in Figure 2 (a), all of the diffraction peaks could be indexed to the orthorhombic SnSe structure with a cell unit of a = 11.50 Å, b = 4.15 Å, and c = 4.44 Å (PDF 48-1244, *Pnma* (62)). For the detailed crystal structure and crystal quality of the synthesized products to be obtained, the layered spiral-type SnSe nanoplates were characterized by transmission electron microscopy (TEM), energy-dispersive X-ray spectroscopy (EDX, AMETEK), and selected-area electron diffraction (SAED). Figure 2 (b) shows a typical low-magnification TEM image of the layered spiral-type SnSe nanoplates transferred onto the TEM grids. The layered spiral-type SnSe nanoplates

DOI: 10.1021/acs.cgd.5b01708
Cryst. Growth Des. XXXX, XXX, XXX−XXX

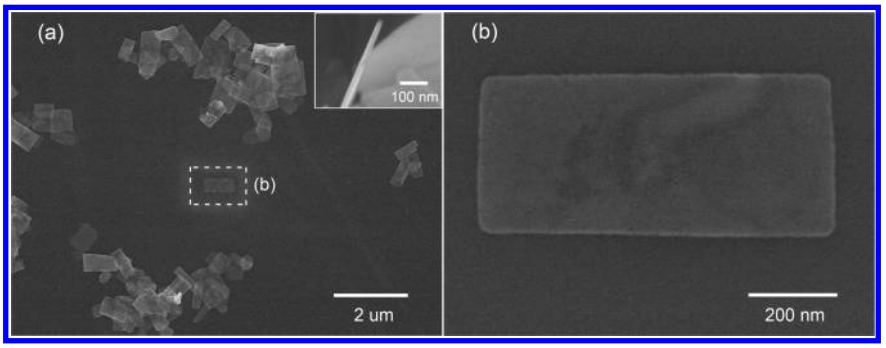

Figure 4. (a) Low-magnification SEM image of SnSe nanoplates obtained with a concentration 2 times higher than that of the standard precursor; upright nanoplates are shown in the upper right corner. (b) High-magnification SEM image of a representative SnSe nanoplate shown in (a) with a dashed square.

are relatively stable against electron beam irradiation in a TEM. The spiral features can be clearly identified; the rectangle sheets spiral up layer by layer to the center summit, which are consistent with the results of the SEM and AFM images. Energy-dispersive X-ray (EDX) spectroscopy was carried out to reveal the chemical composition of the white box shown in Figure 2 (b). As illustrated in Figure 2 (c, d), EDX element mapping images indicate that Sn and Se elements were uniformly distributed, confirming the uniform chemical distribution along the entire nanoplate. Moreover, the corresponding EDX spectrum (Figure 2 (e)) shows a Sn/Se atomic ratio of 1.34:1.37.

The high-resolution TEM (HR-TEM) image of the square area marked in Figure 2 (b) shows clear orthogonal lattice fringes with lattice spacing of ~0.30 nm. The intersection angle of the lattice fringes is approximately 94°(Figure 2(f)), which is in good agreement with the angle between the planes of (011) and $(0\bar{1}1)$ of the orthorhombic SnSe crystal structure.[30,31] Furthermore, the SAED data (Figure 2 (g)), taken from an individual SnSe nanoplate, exhibits a clear orthogonally symmetric spot pattern, indicating the single-crystal nature of the sample. On the other hand, at the center of the nanoplate shown in Figure 2 (b), a hollow core was observed clearly as illustrated in Figure 2 (h), which further proves the helical structure of the nanoplates. In addition, herringbone contours and spiral arms around the hollow core were also found. These results further confirm that a nanoplate is the spiral-type structure grown by the SDD mechanism. Therefore, it can be concluded that the SnSe nanoplates exhibited a layered spiral-type structure with high crystal quality.

The optical absorption behavior of the as-synthesized products was studied by UV−vis−NIR spectroscopy in the region of 400−1600 nm. Figure 3 (a) shows the absorption spectrum of the layered spiral-type SnSe nanoplates, indicating a good absorption from the near-infrared spectrum to the visible-light region. Because of their wide-range absorption region, they have attracted intense attention for application in solar cells, photodetectors, and near-infrared optoelectronic devices. Furthermore, Raman spectroscopy was also performed to investigate the quality of the layered spiral-type SnSe nanoplates. As illustrated in Figure 3 (b), four characteristic peaks at 70.0, 105.5, 127.7, and 148.2 cm^{-1} are clearly observed. The Raman peak at 105.5 cm^{-1} belongs to the B3g phonon mode, which originates from the rigid shear mode of a layer with respect to its neighbors in the *c* direction. On the other hand, the Raman peaks at 70.0, 127.7, and 148.2 cm^{-1} correspond to Ag phonon modes, which come from the planar vibration modes of SnSe in the *b* direction. The Raman peak at 105.5 cm^{-1} has the highest intensity, indicating the layer structure of the SnSe nanoplates. Furthermore, all of the Raman peaks are consistent with those previously reported,[32] indicating that the layered spiral-type SnSe nanoplates have a high quality.

Furthermore, considering that tuning of the supersaturation to a higher level could possibly lead to other growth modes, such as LBL growth, we increased the concentration of the precursors. When the concentration of the precursors was increased by a factor of 2 with respect to the standard synthesis, the nanoplates were obtained as shown from the SEM image in Figure 4. All of the nanoplates are smooth with a rectangular shape, indicating growth in the layer-by-layer mode. In addition, the nanoplates are approximately 1 μm in length with a thickness of approximately 21 nm (as indicated from some upright nanoplates shown in the upper right corner of Figure 4(a)). Therefore, the SDD growth mode can be easily tuned to the layer-by-layer growth mode by manipulating the precursor concentration.

4. CONCLUSIONS

Layered spiral-type SnSe nanoplates with atomically thin helical periodicity were synthesized for the first time through the SDD growth mode. The spirals are composed of four connected SnSe layers with decreasing areas: each basal plane has a rectangular shape and shrinks gradually to the summit when spiraling up. Herringbone contours, spiral arms, and hollow cores exist and further confirm the unique structure and growth mode. In addition, the SDD growth mode can be easily tuned to the layer-by-layer growth mode by manipulating the precursor concentration. The results may hopefully be guidance to design and synthesize other 2D layered materials and promote their applications.

AUTHOR INFORMATION

Corresponding Author

*E-mail: jyliu@fjnu.edu.cn. Tel: +86-18120795008.

Notes

The authors declare no competing financial interest.

ACKNOWLEDGMENTS

This work was financially supported by the Natural Science Foundation of China (No.11374052), the Natural Science Foundation of Fujian Province of China (2012J01256, 2013J01174), Education Department of Fujian Province

DOI: 10.1021/acs.cgd.5b01708
Cryst. Growth Des. XXXX, XXX, XXX−XXX

(JA15140), and the Science and Technology Project from the Education Department of Fujian Province of China (JB13023).

REFERENCES

(1) Xu, M. S.; Liang, T.; Shi, M. M.; Chen, H. Z. *Chem. Rev.* **2013**, *113*, 3766−3798.
(2) Coleman, J. N.; Lotya, M.; O'Neill, A.; Bergin, S. D.; King, P. J.; Khan, U.; Young, K.; Gaucher, A.; De, S.; Smith, R. J.; Shvets, I. V.; Arora, S. K.; Stanton, G.; Kim, H. Y.; Lee, K.; Kim, G. T.; Duesberg, G. S.; Hallam, T.; Boland, J. J.; Wang, J. J.; Donegan, J. F.; Grunlan, J. C.; Moriarty, G.; Shmeliov, A.; Nicholls, R. J.; Perkins, J. M.; Grieveson, E. M.; Theuwissen, K.; McComb, D. W.; Nellist, P. D.; Nicolosi, V. *Science* **2011**, *331*, 568−571.
(3) Xue, D. J.; Tan, J. H.; Hu, J. S.; Hu, W. P.; Guo, Y. G.; Wan, L. J. *Adv. Mater.* **2012**, *24*, 4528−4533.
(4) Pejova, B.; Grozdanov, I. *Thin Solid Films* **2007**, *515*, 5203−5211.
(5) Antunez, P. D.; Buckley, J. J.; Brutchey, R. L. *Nanoscale* **2011**, *3*, 2399−2411.
(6) Franzman, M. A.; Schlenker, C. W.; Thompson, M. E.; Brutchey, R. L. *J. Am. Chem. Soc.* **2010**, *132*, 4060−4061.
(7) Baumgardner, W. J.; Choi, J. J.; Lim, Y. F.; Hanrath, T. *J. Am. Chem. Soc.* **2010**, *132*, 9519−9521.
(8) Liu, S.; Guo, X. Y.; Li, M. R.; Zhang, W. H.; Liu, X. Y.; Li, C. *Angew. Chem., Int. Ed.* **2011**, *50*, 12050−12053.
(9) Liu, S.; Guo, X.; Li, M.; Zhang, W. H.; Liu, X.; Li, C. *Angew. Chem., Int. Ed.* **2011**, *50*, 12050−3.
(10) Vaughn, D. D.; In, S.-I.; Schaak, R. E. *ACS Nano* **2011**, *5*, 8852−8860.
(11) Li, L.; Chen, Z.; Hu, Y.; Wang, X.; Zhang, T.; Chen, W.; Wang, Q. *J. Am. Chem. Soc.* **2013**, *135*, 1213−6.
(12) Meng, F.; Morin, S. A.; Forticaux, A.; Jin, S. *Acc. Chem. Res.* **2013**, *46*, 1616−1626.
(13) Wang, J. D.; Liu, J. K.; Luo, C. X.; Lu, Y.; Yang, X. H. *Cryst. Growth Des.* **2013**, *13*, 4837−4843.
(14) Bierman, M. J.; Lau, Y. K. A.; Kvit, A. V.; Schmitt, A. L.; Jin, S. *Science* **2008**, *320*, 1060−1063.
(15) Wu, H. Y.; Meng, F.; Li, L. S.; Jin, S.; Zheng, G. F. *ACS Nano* **2012**, *6*, 4461−4468.
(16) Morin, S. A.; Jin, S. *Nano Lett.* **2010**, *10*, 3459−3463.
(17) Meng, F.; Morin, S. A.; Jin, S. *J. Am. Chem. Soc.* **2011**, *133*, 8408−8411.
(18) Morin, S. A.; Bierman, M. J.; Tong, J.; Jin, S. *Science* **2010**, *328*, 476−480.
(19) Meng, F.; Jin, S. *Nano Lett.* **2012**, *12*, 234−239.
(20) Hacialioglu, S.; Meng, F.; Jin, S. *Chem. Commun.* **2012**, *48*, 1174−1176.
(21) Lau, Y. K. A.; Chernak, D. J.; Bierman, M. J.; Jin, S. *J. Am. Chem. Soc.* **2009**, *131*, 16461−16471.
(22) Zhu, J.; Peng, H. L.; Marshall, A. F.; Barnett, D. M.; Nix, W. D.; Cui, Y. *Nat. Nanotechnol.* **2008**, *3*, 477−481.
(23) Iijima, S. *Nature* **1991**, *354*, 56−58.
(24) Morin, S. A.; Forticaux, A.; Bierman, M. J.; Jin, S. *Nano Lett.* **2011**, *11*, 4449−4455.
(25) Zhang, L. M.; Liu, K. H.; Wong, A. B.; Kim, J.; Hong, X. P.; Liu, C.; Cao, T.; Louie, S. G.; Wang, F.; Yang, P. D. *Nano Lett.* **2014**, *14*, 6418−6423.
(26) Chen, L.; Liu, B. L.; Abbas, A. N.; Ma, Y. Q.; Fang, X.; Liu, Y. H.; Zhou, C. W. *ACS Nano* **2014**, *8*, 11543−11551.
(27) Xia, J.; Zhu, D.; Wang, L.; Huang, B.; Huang, X.; Meng, X.-M. *Adv. Funct. Mater.* **2015**, *25*, 4255−4261.
(28) Zhuang, A.; Li, J. J.; Wang, Y. C.; Wen, X.; Lin, Y.; Xiang, B.; Wang, X. P.; Zeng, J. *Angew. Chem., Int. Ed.* **2014**, *53*, 6425−6429.
(29) Forticaux, A.; Dang, L. N.; Liang, H. F.; Jin, S. *Nano Lett.* **2015**, *15*, 3403−3409.
(30) Ma, X.-H.; Cho, K.-H.; Sung, Y.-M. *CrystEngComm* **2014**, *16*, 5080−5086.
(31) Car, R.; Ciucci, G.; Quartapelle, L. *Phys. Status Solidi B* **1978**, *86*, 471−478.
(32) Zhao, S.; Wang, H.; Zhou, Y.; Liao, L.; Jiang, Y.; Yang, X.; Chen, G.; Lin, M.; Wang, Y.; Peng, H.; Liu, Z. *Nano Res.* **2015**, *8*, 288−295.

DOI: 10.1021/acs.cgd.5b01708
Cryst. Growth Des. XXXX, XXX, XXX−XXX